

Phase-field modeling of effect of Ni on formation and phase transformation of Cu-rich phase in Fe-Cu-Ni alloys

Ming-Guang Wei(位明光), Zhong-Wen Zhang(张中文), Min Cui(崔敏), Yuan-Bin Zhang(张元彬), and Tong-Guang Zhai(翟同广)

Citation: Chin. Phys. B, 2025, 34 (**8**): 088103. DOI: 10.1088/1674-1056/add501
http://cpb.iphy.ac.cn; http://iopscience.iop.org/cpb

What follows is a list of articles you may be interested in

Parameter calculation and result storage for phase-field simulation in α-Mg dendrite growth of Mg-5-wt% Zn alloy

Wei-Peng Chen(陈伟鹏), Hua Hou(侯华), Yun-Tao Zhang(张云涛), Wei Liu(柳伟), and Yu-Hong Zhao(赵宇宏)
Chin. Phys. B, 2023, 32 (**11**): 118103. DOI: 10.1088/1674-1056/acd7e3

Phase-field study of spinodal decomposition under effect of grain boundary

Ying-Yuan Deng(邓英远), Can Guo(郭灿), Jin-Cheng Wang(王锦程), Qian Liu(刘倩), Yu-Ping Zhao(赵玉平), and Qing Yang(杨卿)
Chin. Phys. B, 2021, 30 (**8**): 088101. DOI: 10.1088/1674-1056/abea9b

Controllable preparation of tungsten/tungsten carbide nanowires or nanodots in nanostructured carbon with hollow macroporous core/mesoporous shell

Xiao-Na Ren(任晓娜), Min Xia(夏敏), Qing-Zhi Yan(燕青芝), Chang-Chun Ge(葛昌纯)
Chin. Phys. B, 2017, 26 (**3**): 038103. DOI: 10.1088/1674-1056/26/3/038103

Cyclic stress induced phase transformation insuper-bainitic microstructure

Wencui Xiu(修文翠), Ying Han(韩英), Cheng Liu(刘澄), Hua Wu(吴化), Yunxu Liu(刘云旭)
Chin. Phys. B, 2017, 26 (**3**): 038101. DOI: 10.1088/1674-1056/26/3/038101

Perfect spin filtering controlled by an electric field in a bilayer graphene junction: Effect of layer-dependent exchange energy

Kitakorn Jatiyanon, I-Ming Tang, Bumned Soodchomshom
Chin. Phys. B, 2016, 25 (**7**): 078104. DOI: 10.1088/1674-1056/25/7/078104

Phase-field modeling of effect of Ni on formation and phase transformation of Cu-rich phase in Fe–Cu–Ni alloys

Ming-Guang Wei(位明光)[1], Zhong-Wen Zhang(张中文)[1], Min Cui(崔敏)[2], Yuan-Bin Zhang(张元彬)[2], and Tong-Guang Zhai(翟同广)[2,†]

[1] *School of Physics Science and Technology, Guangxi University, Nanning* 530004, *China*
[2] *School of Materials Science and Engineering, Shandong Jianzhu University, Jinan* 250101, *China*

(Received 4 March 2025; revised manuscript received 28 April 2025; accepted manuscript online 7 May 2025)

A phase-field model integrated with the thermodynamic databases was constructed to investigate the impact of Ni content on the precipitation kinetics and phase transformation of the Cu-rich phase in Fe–Cu–Ni alloy at 773 K. The results demonstrated that the Cu core–Ni shell structures form via the decomposition of Cu–Ni co-clusters, which is consistent with previous experimental results. As the Ni content increases, both the volume fraction and number density of Cu-rich precipitates increase, while their size decreases. With the increase in Ni content, the transformation from α Cu to 9R Cu is accelerated, which is the opposite to the result of increasing Mn content. Magnetic energy can increase the nucleation rate of the Cu-rich phase, but it does not affect the phase transformation driving force required for its crystal structure transformation.

Keywords: phase-field method, Cu-rich phase, phase transformation, magnetic energy

PACS: 81.10.Jt, 61.50.Ah, 64.70.kd

DOI: 10.1088/1674-1056/add501 **CSTR:** 32038.14.CPB.add501

1. Introduction

Fe–Cu alloys are known for their low cost, excellent weldability, corrosion resistance, and high strength, making them ideal structural materials for fuel cells, shipbuilding, and automotive industries.[1–5] The antimicrobial properties and high strength of Fe–Cu alloys are derived from the precipitation of a Cu-rich phase during the aging process.[6–10] However, the crystal structure of the Cu-rich phase undergoes complex changes during prolonged high-temperature service, resulting in a decrease in the yield strength of Fe–Cu alloy.[11–14] At present, it has been determined that a bcc α-Cu phase is first precipitated in the α-Fe matrix, which then gradually transforms into a metastable 9R phase, and then finally forms a stable fcc γ-Cu phase.[14–17] However, the factors affecting the phase transformation of the Cu-rich phase are still unclear.

Controlling the alloy composition is an effective method to improve the mechanical properties of Fe–Cu alloys. A large number of experiments have been conducted to study the effects of different alloying elements (Mn, Ni, and Al) on the precipitation of the Cu-rich phase.[18–28] However, the influence of Ni on the precipitation of the Cu-rich phase remains a topic of debate. Results of 3-D atom probe tomography analysis indicate that the addition of Ni significantly decreases the nucleation number of the Cu-rich phase.[29] In contrast, some studies have shown that Ni markedly enhances the nucleation rate of the Cu-rich phase.[4,30] So far, there is no consensus on this issue. In addition, the effects of Ni on the phase transformation of the Cu-rich phase remain unclear. As is well known, the influence of a Cu-rich phase with different crystal structures on the mechanical properties of Fe–Cu alloys varies. For example, peak aging is caused by a bcc α-Cu phase that is fully coherent with an α-Fe matrix, but when it transforms into the fcc γ-Cu phase, the Vickers hardness and yield strength of the material significantly decrease.[13,19] The 9R-Cu phase can improve the hydrogen embrittlement resistance of steels.[14] Therefore, understanding the role of Ni in the phase transformation of the Cu-rich phase is of great significance for improving the mechanical properties of Fe–Cu alloys.

The nucleation, growth, and coarsening of the Cu-rich phase occur simultaneously during the aging process, complicating experimental observations. The phase-field method can reproduce the evolution of the microstructure in real-time, overcoming the limitations of experimental methods, and has been widely applied in fields such as solidification, phase transformation, and spinodal decomposition.[31–34] Numerous studies using the phase-field method have been carried out on the precipitation process of the Cu-rich phase, including the formation of core–shell structures,[35,36] the stability of Cu-rich phase,[37] as well as the impacts of temperature,[31,38] alloying elements,[39–41] and strain[42,43] on the precipitation evolution of the Cu-rich phase. However, in most studies,[35,36,40,43] the selected Cu content (15–20 at.%) is too high, which can alter the nucleation mechanism of Cu-rich phases and thus affect their precipitation kinetics.[33] Addi-

[†]Corresponding author. E-mail: tongguang_zhai@yahoo.com

© 2025 Chinese Physical Society and IOP Publishing Ltd. All rights, including for text and data mining, AI training, and similar technologies, are reserved.

tionally, these studies mainly focus on the nucleation, growth, and coarsening of Cu-rich phases. The factors affecting the phase transformation of the Cu-rich phase are still poorly understood.

In this study, a phase-field model was established to investigate the effect of Ni on the precipitation and phase transformation of the Cu-rich phase in Fe–Cu–Ni alloys during isothermal aging. This study reveals the formation mechanism of the Cu core–Ni shell structure, which can significantly improve the mechanical properties of Fe–Cu alloys. A systematic analysis of the effect of Ni on the nucleation and crystal structure transformation of the Cu-rich phase was conducted, providing theoretical support for the design of high-strength Fe–Cu alloys.

2. Phase-field model

To study the formation and phase transformation (α Cu $\rightarrow$ 9R Cu) of the Cu-rich phase in ternary Fe–Cu–Ni alloys, two sets of field variables need to be defined first: concentration field (c_i) and structural order parameter (S). $i = 1, 2, 3$ correspond to Fe, Cu, and Ni, respectively. $S = 0$ represents the α Cu phase and α-Fe matrix, while $S = 1$ stands for the 9R Cu phase. The matrix phase and the α Cu phase are distinguished by the distribution of Cu composition. Cu-enriched regions represent the α Cu phase, while Cu-depleted regions represent the matrix phase. The total free energy F is a function of c_i, S, and temperature (T)

$$F = \int_V \Big\{ \sum_{i=1}^{3} \frac{1}{2}\kappa_c (\nabla c_i)^2 + \frac{1}{2}\kappa_S (\nabla S)^2 + W g(S) + [1-h(S)]G^{\alpha}(c_i,T) + h(S)G^{9\mathrm{R}}(c_i,T) \Big\} \mathrm{d}V, \quad (1)$$

where κ_c and κ_S stand for the gradient energy parameters, and W represents the barrier height of the phase transformation. $g(S) = S^2(1-S)^2$ and $h(S) = S^2(3-2S)$. G^{α} and $G^{9\mathrm{R}}$ represent the Gibbs free energies of α Cu and 9R Cu, respectively. $G^{9\mathrm{R}}$ is expressed by the equation[38]

$$G^{9\mathrm{R}} = 0.1G^{\alpha} + 0.9G^{\gamma}, \quad (2)$$

where G^{γ} is the Gibbs free energy of γ Cu. The Gibbs free energy (G^{α} and G^{γ}) with a magnetic contribution can be described using the sub-regular solution[36,44]

$$G^{\varphi} = \sum_i G_i^{\varphi} c_i + RT \sum_i c_i \ln c_i + \sum_i \sum_{j>i} L_{i,j} c_i c_j + \sum_i \sum_{j>i} \sum_{k>j} L_{i,j,k} c_i c_j c_k + {}^{\mathrm{m}}G^{\varphi}, \quad (3)$$

where $\varphi = \alpha$ or γ, and $i = 1, 2, 3$ stand for Fe, Cu, and Ni, respectively.

$$G_1^{\alpha} = 0, \quad (4)$$

$$G_2^{\alpha} = 4017 - 1.255T, \quad (5)$$

$$G_3^{\alpha} = 8715.084 - 3.556T, \quad (6)$$

$$G_1^{\gamma} = -1462.4 + 8.282T - 1.15T\ln T + 6.4\times10^{-4}T^2, \quad (7)$$

$$G_2^{\gamma} = G_3^{\gamma} = 0, \quad (8)$$

$$L_{1,2}^{\alpha} = 39257.976 - 4.1498304T, \quad (9)$$

$$L_{1,3}^{\alpha} = -956.63 - 1.28726T + (1789.03 - 1.92912T)(c_1 - c_3), \quad (10)$$

$$L_{2,3}^{\alpha} = 8366 + 2.802T, \quad (11)$$

$$L_{1,2,3}^{\alpha} = 0, \quad (12)$$

$$L_{1,2}^{\gamma} = 48232.565 - 8.6095425T + (8861.8816 - 5.2897513T)(c_2 - c_1), \quad (13)$$

$$L_{1,3}^{\gamma} = -12054.355 + 3.27413T + (11082.1315 - 4.45077T)(c_1 - c_3) - 725.805174(c_1 - c_3)^2, \quad (14)$$

$$L_{2,3}^{\gamma} = 8366 + 2.802T + (-4359.6 + 1.812T)(c_2 - c_3), \quad (15)$$

$$L_{1,2,3}^{\gamma} = -73272 + 30.9T. \quad (16)$$

The magnetic energy (${}^{\mathrm{m}}G^{\varphi}$) in Eq. (3) is defined as[36,44]

$${}^{\mathrm{m}}G^{\varphi} = RT\ln(b^{\varphi}+1) f(\tau), \quad (17)$$

where R represents the gas constant, b^{φ} stands for the average magnetic moment, $\tau = T/T^{\varphi}$, and T^{φ} represents the Curie temperature of ferromagnetic materials.[36,44]

$$b^{\alpha} = 2.22c_1 + 0.85c_3, \quad (18)$$

$$b^{\gamma} = -2.1c_1 + 0.52c_3 + 20c_1c_2c_3 + c_2c_3\Big[-0.7316 - 0.3174(c_2 - c_3)\Big] + c_1c_3\Big[9.55 + 7.23(c_1 - c_3) + 5.93(c_1 - c_3)^2 + 6.18(c_1 - c_3)^3\Big], \quad (19)$$

$$T^{\alpha} = 1043c_1 + 575c_3, \quad (20)$$

$$T^{\gamma} = -201c_1 + 633c_3 + c_1c_3[2133 - 682(c_1 - c_3)] + c_2c_3[-935.5 - 594.9(c_2 - c_3)] + 7000c_1c_2c_3, \quad (21)$$

$$f(\tau) = \begin{cases} 1 - \frac{1}{D}\left\{\frac{79\tau^{-1}}{140p} + \frac{474}{497}\left(\frac{1}{p} - 1\right) \times \left(\frac{\tau^3}{6} + \frac{\tau^9}{135} + \frac{\tau^{15}}{600}\right)\right\}, & (\tau \le 1), \\ -\frac{1}{D}\left(\frac{\tau^{-5}}{10} + \frac{\tau^{-15}}{315} + \frac{\tau^{-25}}{1500}\right), & (\tau > 1), \end{cases} \quad (22)$$

$$D = \frac{518}{1125} + \frac{11692}{15975}\left(\frac{1}{p} - 1\right), \quad (23)$$

where the values of p in α Cu and γ Cu are 0.4 and 0.28, respectively.

The concentration evolution of different solutes and the phase transformation of the Cu-rich phase can be obtained by solving the Allen–Cahn[45] equation and the Cahn–Hilliard[46] equation

$$\frac{\partial S(r,t)}{\partial t} = -L \cdot \frac{\delta F}{\delta S(r,t)} + \xi_S(r,t), \quad (24)$$

$$\frac{\partial c_i(r,t)}{\partial t} = \nabla \cdot M_i \cdot \nabla \frac{\delta F}{\delta c_i(r,t)} + \xi_c(r,t), \tag{25}$$

where r is the spatial position and t is the simulation time. L is the kinetic coefficient and ξ represents the random noise terms.[47] M_i is the diffusion mobility of different solute atoms, defined as

$$M_i = c_{0i}(1-c_{0i})\left\{(1-S)\frac{D_i^{\alpha}(T)}{RT} + S\frac{D_i^{\gamma}(T)}{RT}\right\}, \tag{26}$$

where c_{0i} is the initial concentration and D_i^{φ} is the diffusion coefficient.

The size of the selected simulation area in this study is $64\,\mathrm{d}x \times 64\,\mathrm{d}x \times 64\,\mathrm{d}x$ (grid size: $\mathrm{d}x = 0.5 \times 10^{-9}$ m). Periodic boundary conditions are applied. The Ni content in Fe–1Cu–Ni (at.%) ternary alloys is set to 0.5 at.%, 1.5 at.%, and 3 at.%. The energy was normalized by dividing it by RT. Aging time $t = t^*(l^2/D_{\mathrm{Cu}}^{\alpha})$, $t^* = n\Delta t$, where n is the number of iterations, $\Delta t = 0.01$ is the time step, $l = 0.5$ nm is the characteristic length,[42] and $D_{\mathrm{Cu}}^{\alpha} = 1.5 \times 10^{-21}$ m^2/s is the diffusion coefficient of the Cu atom in an α-Fe matrix at 773 K. The parameter values required for the phase-field simulation are listed in Table 1.

Table 1. Simulation parameters.[36–38]

Parameter	Value
T (K)	773
R (J·mol^{-1}·K^{-1})	8.314
V_m (m^3/mol)	7.09×10^{-6}
W (J·mol^{-1})	5.0×10^3
κ_c (J·m^{2}mol^{-1})	5.0×10^{-15}
κ_S (J·m^2·mol^{-1})	1.0×10^{-15}
$D_i^{\varphi} = {}^0D_i^{\varphi}\exp(-Q_i^{\varphi}/RT)$	${}^0D_{\mathrm{Cu}}^{\alpha} = 4.7 \times 10^{-5}$, $D_{\mathrm{Cu}}^{\gamma} = 4.3 \times 10^{-5}$
${}^0D_i^{\varphi}$ (m^2/s)	${}^0D_{\mathrm{Ni}}^{\alpha} = 1.49 \times 10^{-4}$, $D_{\mathrm{Ni}}^{\gamma} = 1.78 \times 10^{-5}$
Q_i^{φ} (J/mol)	$Q_{\mathrm{Cu}}^{\alpha} = 2.44 \times 10^5$, $Q_{\mathrm{Cu}}^{\gamma} = 2.8 \times 10^5$
	$Q_{\mathrm{Ni}}^{\alpha} = 2.33 \times 10^5$, $Q_{\mathrm{Ni}}^{\gamma} = 2.64 \times 10^5$

3. Results and discussion

3.1. The formation process of Cu core–Ni shell structures

Figure 1 shows the compositional evolution during the Cu core–Ni shell structure formation process in the Fe–1Cu–1.5Ni (at.%) alloy at 773 K. During the initial aging stage, Cu-rich and Ni-rich clusters were gradually precipitated in the matrix under the influence of compositional fluctuations (see Figs. 1(d) and 1(g)). A closer examination reveals that their nucleation sites are the same. Owing to the complete overlap of Cu-rich and Ni-rich regions, the early precipitates can be identified as the Cu–Ni co-clusters, which aligns with previous reports.[3,19] With the growth of the co-clusters, Ni atoms within the clusters were gradually expelled and enriched at the interface between the Cu-rich clusters and the matrix, forming a core–shell structure, which is also consistent with the experimental results.[19] The formation of the core–shell structure might be related to the mixing enthalpy (ME) between Cu, Ni, and Fe. $\mathrm{ME_{CuNi}} = +4$ kJ/mol and $\mathrm{ME_{CuFe}} = +13$ kJ/mol.[48] When ME > 0, it means that there is a tendency for separation between the two types of atoms. Due to $\mathrm{ME_{CuNi}} < \mathrm{ME_{CuFe}}$, the separation between Cu and Fe is easier. Additionally, the co-clusters could reduce the nucleation energy barrier, promoting the nucleation of Cu-rich phase.[39,49] Therefore, Cu–Ni co-clusters were preferentially precipitated. As the co-clusters grow, Cu–Ni co-clusters gradually decompose under the effect of mixing enthalpy, with Ni atoms segregating at the interface, and eventually forming a Cu core–Ni shell structure.[19] First-principles calculations[50] also indicated that Ni was energetically favored to be located at the interface between the cluster and the matrix rather than in the center of the cluster.

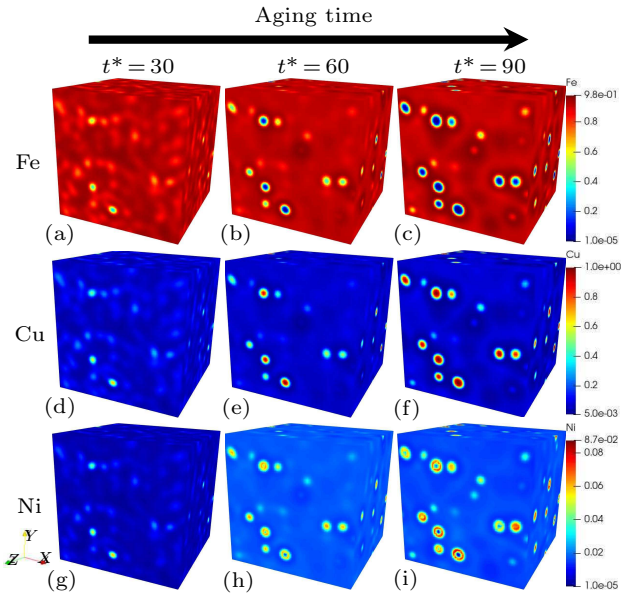


Fig. 1. Temporal evolution of composition fields for Fe, Cu, and Ni in the Fe–1Cu–1.5Ni (at.%) alloy aged at 773 K.

3.2. Effect of Ni on the precipitation of the Cu-rich phase

Figure 2 shows the precipitation evolution of Cu-rich precipitates in Fe–1Cu–xNi ($x = 0.5$, 1.5, and 3) alloy during isothermal aging at 773 K. Within the simulation region, the red spheres denote the precipitated Cu-rich phase, and the blue region corresponds to the α-Fe matrix. At $t^* = 30$, relatively few Cu-rich phases are randomly dispersed in the matrix in the Fe–1Cu–0.5Ni alloy, as shown in Fig. 2(a). As aging progresses, both the number density and size of the Cu-rich phase increase significantly. With increasing Ni content, the nucleation rate of the Cu-rich phase noticeably increases within the same time, thereby increasing the number density of the Cu-rich phase. This could be attributed to the nucleation energy barrier that needs to be overcome for Cu-rich phase formation decreasing with the increase of the Ni content.[39,49]

To quantify the effect of Ni on the precipitation kinetics of the Cu-rich phase, the evolution of volume fraction, number density, and average radius of the Cu-rich phase with aging

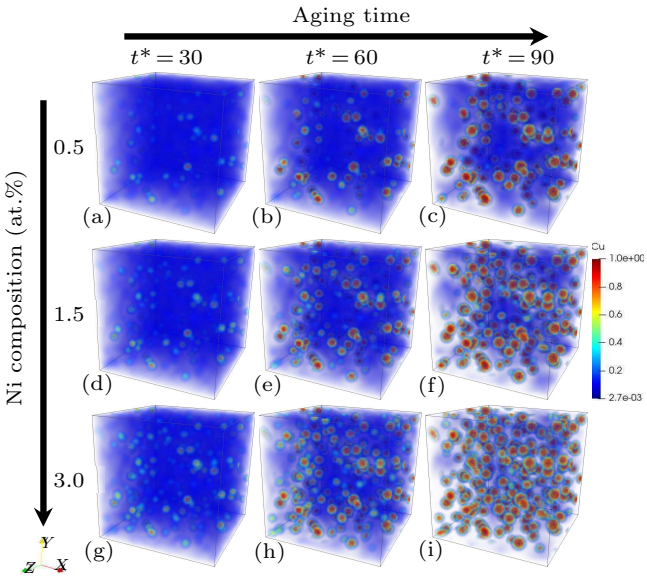


Fig. 2. Morphological evolution of the Cu-rich phase in Fe–1Cu–*x*Ni ($x = 0.5$, 1.5, and 3) alloys aged at 773 K as a function of aging times.

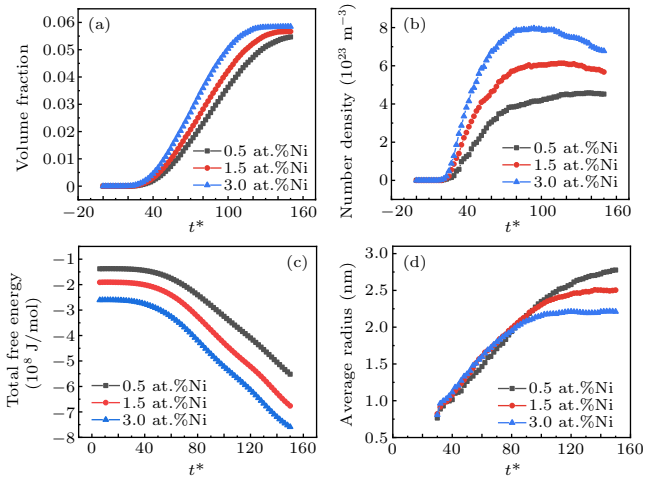


Fig. 3. The variations of (a) volume fraction, (b) number density, (c) total free energy, and (d) average radius of Cu-rich precipitates with aging time in Fe–1Cu–*x*Ni alloys ($x = 0.5$, 1.5 and 3).

time are shown in Fig. 3. With the increase in Ni, the volume fraction curve shifts noticeably to the left, and the stable value of the volume fraction increases significantly, as shown in Fig. 3(a). The number density of the Cu-rich phase first increases dramatically, and then decreases after reaching its peak value, as shown in Fig. 3(b). When the Ni content increases from 0.5 at.% to 3 at.%, the peak number density of the Cu-rich phase increases by 1.8 times. This is because as the amount of Ni increases, the nucleation barrier to be overcome in the Cu-rich phase formation decreases, which increases the nucleation density of the Cu-rich phase.[39,49] Meanwhile, as Ni content increases, the decrease in total free energy becomes more pronounced (see Fig. 3(c)), which suggests a larger nucleation driving force for the Cu-rich phase. Therefore, the nucleation rate of the Cu-rich phase increases with the rising Ni content. The variation of the size of the Cu-rich phase is illustrated in Fig. 3(d). At the early stages of aging, the size of the Cu-rich phase increases gradually as the Ni content rises. When the Ni composition is fixed, the final size of the Cu-rich phase stabilizes over time, whereas at a fixed time, higher Ni content leads to a reduction in precipitate size. This is because as the Ni content increases, the nucleation driving force of the Cu-rich phase increases, which accelerates the growth of Cu–Ni co-clusters at the early aging stage. However, as the co-clusters grow, the Ni atoms are segregated at the interface between the Cu-rich phase and the α-Fe phase, forming a Ni-rich shell. The Ni-rich shell could serve as a diffusion barrier, inhibiting the growth of the Cu-rich phase.[19] Jiao *et al.*[4] found that as the Ni content increases, the radius of the Cu-rich phase decreases from 4 nm to 2 nm, while its number density increases, resulting in a substantial increase in the ultimate tensile strength of Fe–Cu–Ni steel to 1.26 GPa. Shen *et al.*[51] also observed a similar phenomenon. This is consistent with our simulation results, indicating that an increased Ni content effectively enhances the mechanical properties of Fe–Cu alloys.

3.3. Effect of Ni on the phase transformation of the Cu-rich phase

Figure 4 shows the effect of Ni on the phase transformation from α Cu to 9R Cu in the Fe–Cu–Ni alloys aged at 773 K. When the Ni content is 0.5 at.%, the formed Cu-rich precipitates were all the α Cu phase before $t^* = 120$, as shown by the orange circles in Fig. 4(b). When $t^* = 120$, only a small amount of α Cu completely transforms into the 9R Cu phase. With the increase in Ni content, the incubation period for the phase transformation of the Cu-rich phase is significantly shortened. At $t^* = 100$, a large amount of α Cu transforms into the 9R Cu phase in the alloy with a Ni content of 3 at.%. This indicates that an increased Ni content promotes the crystal structure transformation of the Cu-rich phase, which is the opposite of the result observed with the addition of Mn.[41] The critical nucleation radius of 9R Cu decreases gradually as the Ni content increases (see Fig. 5).

To further reveal the effect of Ni on the transformation of α Cu into 9R Cu, figure 6 illustrates the variation of Gibbs free energy of the two phases with Ni content. When the Cu content is low, the free energy of 9R Cu is greater than that of α Cu, which means that α Cu is more energetically stable than 9R Cu. Therefore, the α Cu phase was first precipitated. As the Cu atoms are gradually enriched into the α Cu phase, the Gibbs free energy of 9R Cu gradually becomes smaller than that of α Cu. This indicates that 9R Cu is more stable, and consequently, α Cu will eventually transform into 9R Cu. The energetically preferred composition of 9R Cu is shown to be significantly sensitive to changes in Ni content. In Fe–1Cu–0.5Ni alloy, when the Cu content reaches 0.188, the Gibbs free energy of α Cu begins to exceed that of 9R Cu. As

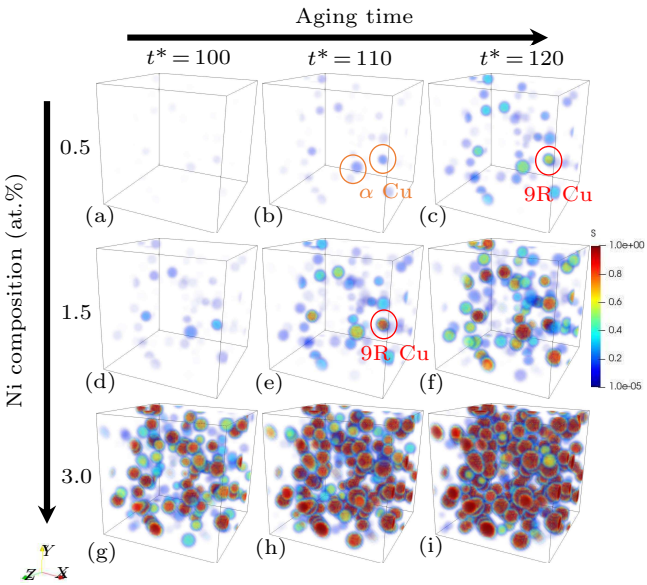


Fig. 4. Structural phase transformation of the Cu-rich phase in Fe–1Cu–*x*Ni alloys ($x = 0.5$, 1.5 and 3) at 773 K.

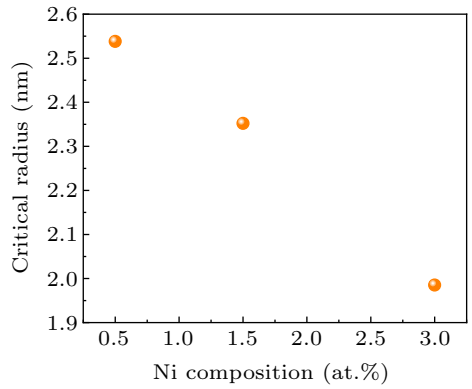


Fig. 5. Critical radius of the α Cu to 9R Cu phase transformation in alloys with different Ni compositions.

the Ni content increases to 3 at.%, this critical Cu content decreases to 0.125 (see Figs. 6(a) and 6(c)). The driving force for the phase transformation originates from the free energy difference between α Cu and 9R Cu (i.e., $\Delta G = G^{9R} - G^{\alpha}$). As the Cu content increases, ΔG continues to decrease, and the higher the Ni content in the alloys, the greater the magnitude of the decrease, as shown in Fig. 7(a). This suggests that the phase transformation driving force strengthens with increasing Ni content. When the Cu content is less than the critical composition, $\Delta G > 0$, which means that α Cu is more stable energetically and cannot spontaneously transform into 9R Cu. However, once the Cu content exceeds the critical composition, $\Delta G < 0$, α Cu can gradually transform into the 9R Cu. As the Ni content increases, the critical Cu composition gradually decreases, thereby promoting the spontaneous transformation from α Cu to 9R Cu. Since the phase transformation (α Cu $\rightarrow$ 9R Cu/γ Cu) occurs after the Cu concentration reaches 100 at.% (i.e., pure Cu),[38,52] the Ni content plays a significant role in the change of the phase transformation driving force for pure Cu, as shown in Fig. 7(b). It is readily seen that as the Ni content increases, the driving force increases, accelerating the transformation from α Cu to 9R Cu. By comparing the effects of Ni and Mn on the driving force for phase transformation, it can be concluded that the driving force provided by Ni is consistently greater than that provided by Mn. As the Ni content increases, the phase transformation driving force gradually strengthens, promoting the occurrence of phase transformation. However, an increase in Mn content leads to a gradual reduction in the driving force, thereby inhibiting the transformation of the Cu-rich phase, which is exactly opposite to the effect of Ni (see Fig. 7(b)).[41,53]

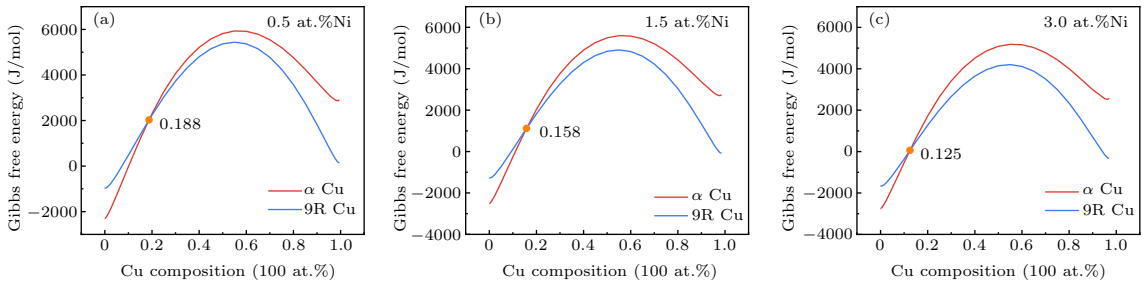


Fig. 6. Gibbs free energies of α Cu and 9R Cu phases in the Fe–Cu–Ni alloys with different Ni compositions at 773 K: (a) 0.5 at.%, (b) 1.5 at.%, and (c) 3.0 at.%.

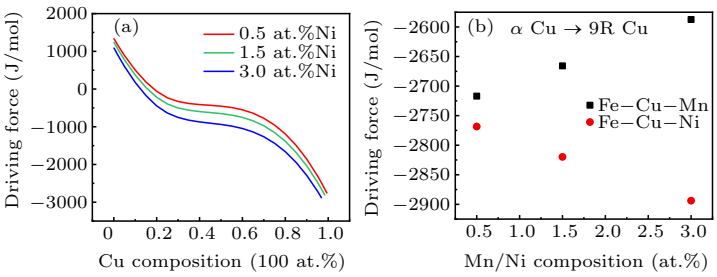


Fig. 7. (a) Variation curves of phase transformation driving force (α Cu $\rightarrow$ 9R Cu) with Cu composition in alloys with different Ni contents. (b) Variation of driving force of phase transformation in pure Cu with Ni and Mn content.

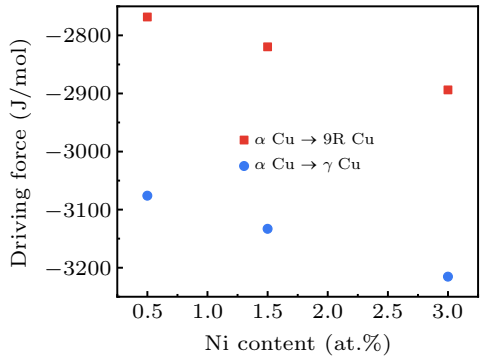


Fig. 8. Variation of the driving forces of α Cu to 9R/γ Cu transformation with Ni content.

Figure 8 illustrates the effect of Ni on the driving force for the transformation of α Cu to 9R/γ Cu. The driving force required for the precipitation of 9R Cu is relatively low compared to γ Cu. As a result, α Cu preferentially transitions to 9R Cu, and then gradually transitions to γ Cu, which is consistent with the experimental results.[16]

3.4. Effect of magnetic energy on the formation of the Cu-rich phase

Figure 9 shows the influence of magnetic energy on the precipitation process of the Cu-rich phase. It is easy to observe that magnetic energy can drastically increase the nucleation rate of Cu-rich phases compared to the case where magnetic energy is not considered. This is attributed to the introduction of magnetic energy, which further reduces the total free energy, providing a greater driving force for the nucleation of the Cu-rich precipitates, thereby accelerating their precipitation. However, as the Ni content increases, the contribution of magnetic energy to the driving force gradually decreases (see Fig. 10(a)). By calculating the effect of magnetic energy on the phase transformation driving force from α Cu to 9R Cu, as shown in Fig. 10(b), it is found that magnetic energy does not alter the magnitude of the driving force for the phase transition of the Cu-rich phase. Additionally, the magnetic energy can also influence the nucleation mechanism of the Cu-rich phase. The Cu-rich phase typically precipitates through two mechanisms: nucleation and growth and pseudo-spinodal decomposition.[33,38] As shown in Fig. 11, magnetic energy has a significant impact on the critical values of these two nucleation mechanisms. When the contribution of magnetic energy is considered, the critical Cu content required for the precipitation of the Cu-rich phase via spinodal decomposition is also significantly reduced from 9.88 at.% to 7.38 at.%. This means that when the Cu-rich phase precipitates, the nucleation energy barrier that needs to be overcome is also reduced, which is more favorable for the nucleation of the Cu-rich phase.

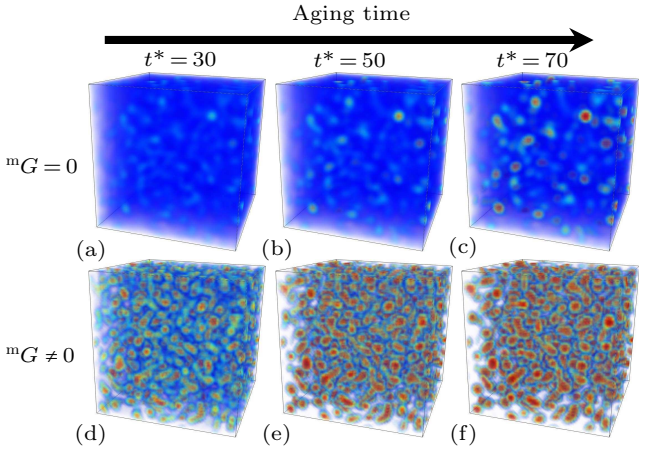


Fig. 9. The precipitation of the Cu-rich phase in Fe–1Cu–5Ni alloy under magnetic energy (^mG) at 773 K.

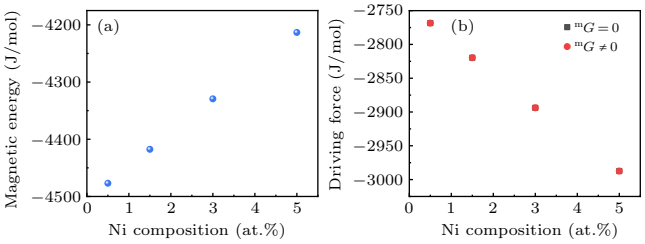


Fig. 10. (a) The variation of magnetic energy with Ni content. (b) The influence of magnetic energy on the driving force of phase transformation.

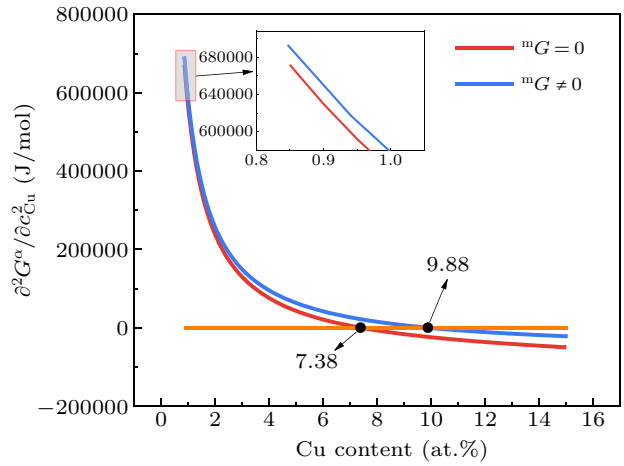


Fig. 11. The second derivative of the free energy of α Cu phase (G^α) under magnetic energy.

4. Conclusion

A phase field model was employed to uncover the impact of Ni on the formation and phase transformation of the Cu-rich phase. Several conclusions are yielded. (1) The Ni–Cu co-clusters decompose to form the Cu core–Ni shell structure, which is consistent with the experimental report. (2) Increasing the Ni content can effectively increase the volume fraction and number density of the Cu-rich phase, and significantly inhibit the coarsening of the Cu-rich phase during the later stages of aging, thus enhancing the precipitation strengthening of the Cu-rich phase. (3) As the Ni content increases, the driving force for phase transformation increases, which reduces both

the time and critical radius required for the transformation of the α Cu phase to the 9R phase. (4) Magnetic energy reduces the incubation time of the Cu-rich phase and increases its nucleation rate, but has no effect on the driving force for the phase transition of the Cu-rich phase. Moreover, magnetic energy reduces the critical composition between different formation mechanisms of the Cu-rich phase.

Acknowledgment

Project supported by the National Natural Science Foundation of China (Grant No. 51871086).

References

[1] Jiang M, Han Y, Sun J, Zu G, Zhu W, Zhao Y, Chen H and Ran X 2022 *Mater. Design* **221** 110977
[2] Isheim D, Kolli R P, Fine M E and Seidman D N 2006 *Scripta Mater.* **55** 35
[3] Konstantinović M J, Uytdenhouwen I, Bonny G, Castin N, Malerba L and Efsing P 2019 *Acta Mater.* **179** 183
[4] Jiao Z B, Luan J H, Zhang Z W, Miller M K, Ma W B and Liu C T 2013 *Acta Mater.* **61** 5996
[5] Dhua S K, Mukerjee D and Sarma D S 2001 *Metall. Mater. Trans. A* **32** 2259
[6] Jiang J, Xu D, Xi T Shahzad M B, Khan M S, Zhao J, Fan X, Yang C, Gu T and Yang K 2016 *Corros. Sci.* **113** 46
[7] Xi T, Shahzad M B, Xu D, Zhao J, Yang C, Qi M and Yang K 2016 *Mater. Sci. Eng. A-Struct.* **675** 243
[8] Kapoor M, Isheim D, Vaynman S, Fine M E and Chung Y W 2016 *Acta Mater.* **104** 166
[9] Wang H, Gao X, Chen S, Li Y, Wu Z and Ren H 2020 *J. Alloys Compd.* **846** 156386
[10] Jiang M, Han Y, Chen X, Zu G, Zhu W and Ran X 2022 *J. Mater. Sci. Technol.* **121** 93
[11] Worrall G M, Buswell J T, English C A, Hetherington M G and Smith G D W 1987 *J. Nucl. Mater.* **148** 107
[12] Holzer I and Kozeschnik E 2010 *Mat. Sci. Eng. A-Struct.* **527** 3546
[13] Nizinkovskyi R, Halle T and Krüger M 2022 *J. Nucl. Mater.* **566** 153764
[14] Sun H, Lv W, Yang Y, Li D, Yan L, Pang X, He Y and Gao K 2023 *Acta Mater.* **246** 118722
[15] Han G, Xie Z J, Li Z Y, Lei B, Shang C J and Misra R D K 2017 *Mater. Design* **135** 92
[16] Othen P J, Jenkins M L and Smith G D W 1994 *Phil. Mag.* **70** 1
[17] Monzen R, Iguchi M and Jenkins M L 2000 *Phil. Mag. Lett.* **80** 137
[18] Vaynman S, Isheim D, Prakash Kolli R, Bhat S P, Seidman D N and Fine M E 2008 *Metall. Mater. Trans. A* **39** 363
[19] Wen Y R, Hirata A, Zhang Z W, Fujita T, Liu C T, Jiang J H and Chen M W 2013 *Acta Mater.* **61** 2133
[20] Zhang C, Enomoto M, Yamashita T and Sano N 2004 *Metall. Mater. Trans. A* **35** 1263
[21] Maury F, Lorenzelli N and De Novion C H 1991 *J. Nucl. Mater.* **183** 217
[22] Osamura K, Okuda H, Asano K, Furusaka M, Kishida K, Kurosawa F and Uemori R 1994 *ISIJ Int.* **34** 346
[23] Isheim D, Gagliano M S, Fine M E and Seidman D N 2006 *Acta Mater.* **54** 841
[24] Kolli R P, Mao Z, Seidman D N and Keane D T 2007 *Appl. Phys. Lett.* **91** 241903
[25] Kolli R P and Seidman D N 2008 *Acta Mater.* **56** 2073
[26] Kapoor M, Isheim D, Ghosh G, Vaynman S, Fine M E and Chung Y W 2014 *Acta Mater.* **73** 56
[27] Gorbatov O I, Gornostyrev Y N, Korzhavyi P A and Ruban A V 2015 *Scripta Mater.* **102** 11
[28] Vincent E, Becquart C S and Domain C 2006 *J. Nucl. Mater.* **351** 88
[29] Li T, Xiong X Y, Shen Q, Wang X J, Li J B and Liu W Q 2019 *Mater. Res. Express* **6** 106510
[30] Wang Z, Du X, Li T, Sun K, Tong X, Li M, Liu R, Liu Y and Chen D 2022 *J. Nucl. Mater.* **562** 153601
[31] Wang K, Wei M, Liao Z, Jin S, Wan B, Lei Z and Li W 2023 *J. Alloys Compd.* **952** 170052
[32] Wei M, Zhai T, Wang Y, Zhang Z, Wang K and Zhang C 2024 *J. Mater. Res. Technol.* **31** 2618
[33] Wei M, Zhai T and Wang K 2024 *J. Mater. Res. Technol.* **33** 8983
[34] Chen Z H, Sheng J, Liu Y, Shi X M, Huang H B, Xu K, Wang C Y, Wu S, Sun B, Liu H F and Song H F 2024 *Chin. Phys. B* **33** 048201
[35] Koyama T and Onodera H 2005 *Mater. Trans.* **46** 1187
[36] Koyama T, Hashimoto K and Onodera H 2006 *Mater. Trans.* **47** 2765
[37] Biner S B, Rao W and Zhang Y 2016 *J. Nucl. Mater.* **468** 9
[38] Zhu J, Zhang T, Yang Y and Liu C T 2019 *Acta Mater.* **166** 560
[39] Li B, Zhang L, Li C, Li Q, Chen J, Shu G, Weng Y, Xu B, Hu S and Liu W 2018 *J. Nucl. Mater.* **507** 59
[40] Sun Y, Zhao Y, Zhao B, Guo Z, Tian X, Yang W and Hou H 2020 *Calphad* **69** 101759
[41] Wei M, Zhai T, Xu Y, Tu Y and Han H 2025 *J. Mater. Res. Technol.* **35** 1971
[42] Zhao Y, Sun Y and Hou H 2022 *Prog. Nat. Sci.* **32** 358
[43] Zhao Y 2022 *J. Mater. Res. Technol.* **21** 546
[44] Dinsdale A T 1991 *Calphad* **15** 317
[45] Allen S M and Cahn J W 1972 *Acta Mater.* **20** 423
[46] Cahn J W and Hilliard J E 1958 *J. Chem. Phys.* **28** 258
[47] Li Y S, Zhu H, Zhang L and Cheng X L 2012 *J. Nucl. Mater.* **429** 13
[48] Jiao Z B, Luan J H, Miller M K, Yu C Y and Liu C T 2015 *Acta Mater.* **84** 283
[49] Zhang C and Enomoto M 2006 *Acta Mater.* **54** 4183
[50] Seko A, Nishitani S R, Tanaka I, Adachi H and Fujita E F 2004 *Calphad* **28** 173
[51] Shen Q, Xiong X Y, Li T, Chen H, Cheng Y M and Liu W Q 2018 *Mat. Sci. Eng. A-Struct.* **723** 279
[52] Kolli R P and Seidman D N 2008 *Acta Mater.* **56** 2073
[53] Sun Y Y, Zhao Y H, Zhao B J, Yang W K, Li X L and Hou H 2019 *J. Mater. Sci.* **54** 11263